Available online at www.sciencedirect.com
ScienceDirect
Journal of Sound and Vibration 306 (2007) 271–283
JOURNAL OF SOUND AND VIBRATION
www.elsevier.com/locate/jsvi

Non-smooth dynamics of spur gears with manufacturing errors

Giorgio Bonori, Francesco Pellicano*

Department of Mechanical and Civil Engineering, University of Modena and Reggio Emilia, Modena, Italy

Received 3 July 2006; received in revised form 26 April 2007; accepted 10 May 2007
Available online 28 June 2007

Abstract

This paper presents a method for analysing nonlinear vibrations of spur gears in presence of manufacturing errors. The approach is based upon the classical one-degree-of-freedom model, with backlash and time varying stiffness. Manufacturing errors are treated stochastically, starting from the knowledge of the gear tolerance class. A random profile error distribution is given for each tooth; then teeth errors are combined in order to span all possible reciprocal teeth contacts. The result is an analytical forcing, in terms of transmission error, which includes statistically the effect of local errors. Finally, a full dynamic analysis is carried out in the case of perfect and imperfect gears, in order to show the effect of profile errors and their variance on the gear vibration.

1. Introduction

Gear noise and vibration were intensively studied in the past; recently, the interest grew because of stronger restrictions of standards regarding the noise level and the increase of international competition.

The transmission error due to teeth deformations is one of the most important sources of vibration and noise in gears; it excites all gearbox components and the vibration propagates along shafts to the external housing. Since the beginning of the previous century, the concept of transmission error was used to describe the displacement-type vibration excitation [1–3]. Mark [4] described the basic theory to provide an analytical expression of the static transmission error, which was considered the main parameter to control the dynamics of gears; it generates a continuous variation of the teeth deflection and an angular transmission error during gears rotation.

Many experiments were carried out in the last 20 years to investigate the correlation between transmission error and gear noise. The strong interaction between noise and static transmission error has been clearly proved [5]; several experiments on gear systems showed that different nonlinear phenomena appear due to the transmission error [6]: multiple coexisting stable motions, sub- and super-harmonic resonances, fold bifurcations, long period sub-harmonic and chaotic motions. Even though there is a general agreement about the nature of the phenomenon, the current understanding of gear vibration remains incomplete.

*Corresponding author. Tel.: +39 59 2056154; fax: +39 59 2056129.
E-mail addresses: bonori.giorgio@unimore.it (G. Bonori), francesco.pellicano@unimore.it (F. Pellicano).

0022-460X/$ - see front matter © 2007 Elsevier Ltd. All rights reserved.
doi:10.1016/j.jsv.2007.05.013

An interesting literature overview can be found in Ref. [7], where the mathematical models used in gear dynamics were classified by considering: the evaluation of the dynamic factor, tooth compliance, gear dynamics, geared rotor dynamics, and torsion vibration.

Important papers were published by Hsu and Cheng [8] and Benton and Seireg [9] who focused their attention to the steady-state response of spur gear systems, in order to detect the effect of parametric excitations on resonances and instabilities.

Many authors proposed different models to study the dynamic effect of clearance in gears. Wang [10,11] defined a backlash function as the angular distance between reverse tooth flanks, while the forward active tooth flank remains in contact; since the backlash depends on the gear angular position, it was considered a time varying function. In the nonlinear model developed by Cai [12] the dynamic loads are forced to zero when tooth pairs are not in contact. Kahraman and Singh [13] considered the effect of backlash and time varying mesh stiffness using the harmonic balance method. Amabili and Rivola [14] obtained a continuous closed form solution for any rotational speed and computed transition curves, stable and unstable regions, by means of the Hill infinite determinant. Many authors [13–18] considered a nonlinear displacement function $f(t)$ to describe the change of stiffness, which is related to the loosing of contact. Tomlinson and Lam [19] showed an application of this technique to an asymmetrical clearance element. Theodossiades and Natsiavas [20] predicted chaotic behaviour: intermittent chaos and boundary crises. Ozguven [21] extended the nonlinear spur gear model considering both shaft and bearing dynamics.

All previous papers agree in considering the following sources of gear vibrations: gear mesh transmission error, impulsive or cyclic drive torque and fluctuations in the output torque demand.

Many authors indicated manufacturing errors as further source of vibration. The first attempt to consider geometrical imperfections was made by Walker [3], who focused his attention to intentional profile modifications, designed to compensate teeth deflections. In 1969, Munro [22] described how geometrical imperfections could significantly alter load and motion transmission. Umezawa et al. [23,24] investigated the influence of the pressure angle, the normal pitch and the waved profile errors on gears vibration. A similar work was proposed by Velex and Maatar [25], they verified the influence of shape deviation and mounting errors on spur or helical gear vibrations. A transfer function approach was proposed in Ref. [26]; this model is able to separate the effects of gear tooth errors and design parameters, it gives a detailed description about the influence of error classes on the static transmission error spectrum.

Refs. [13,27–29] confirmed the importance of considering manufacturing errors in gear dynamics; the possibility of predicting gear quality by means of vibration analysis was shown in Ref. [27].

The analysis of the literature shows that, even though vibrations of gear pairs have been intensively investigated, as well as the effect of manufacturing errors, a systematic and stochastic approach has not yet been developed. Indeed, the nature of errors is not deterministic and gears having the same tolerance could undergo to different types of error excitation.

In the present paper, manufacturing errors are stochastically included in the classical one-degree-of-freedom model with backlash and time varying stiffness. The model includes also deterministic profile modifications such as tip and root relief, which are considered in a finite element analysis that evaluates teeth flexibility.

Manufacturing errors are simulated by generating a random distribution of profile error within the K-chart of the gear; this process is repeated for each tooth of the gear pair. In this way each tooth has different errors, even though the tolerance is the same. Then, all combinations of teeth contacts, giving rise to a specific transmission error, are evaluated and one obtains the global error law in the form of Fourier series.

Finally, an actual test case is considered and a full dynamic analysis is carried out both on perfect and imperfect gear pairs.

2. Equation of motion

The theoretical model considers the spur gear pair as a single-degree-of-freedom lumped system. Each gear is represented by a rigid disk coupled along the line of action through a time varying mesh stiffness $k(t)$ and a

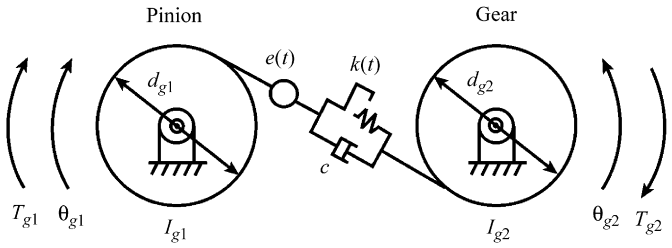

Fig. 1. The spur gear model.

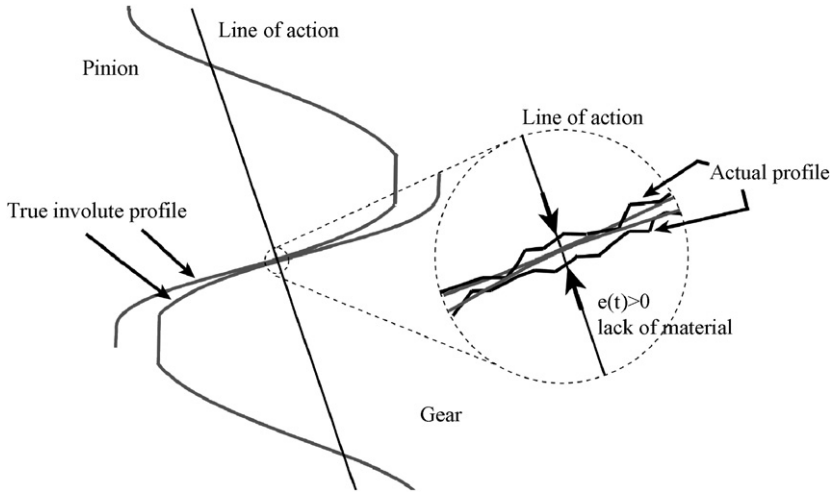

Fig. 2. Manufacturing errors: lack of material along the line of action.

constant mesh damping c (see Fig. 1). The dynamics is governed by the following equation [13]:

$$m_e\ddot{x}(t) + c(\dot{x}(t) - \dot{e}(t)) + k(t)f(x(t) - e(t)) = T_g(t), \tag{1}$$

where m_e is the equivalent mass:

$$m_e = \frac{1}{\left\{(d_{g1}^2/4I_{g1}) + (d_{g2}^2/4I_{g2})\right\}}, \tag{2}$$

T_g is the equivalent applied load:

$$T_g(t) = m_e\left(\frac{d_{g1}T_{g1}(t)}{2I_{g1}} + \frac{d_{g2}T_{g2}(t)}{2I_{g2}}\right), \tag{3}$$

$x(t)$ is the dynamic transmission error (also called DTE) along the line of action:

$$x(t) = \frac{d_{g1}}{2}\theta_{g1}(t) - \frac{d_{g2}}{2}\theta_{g2}(t), \tag{4}$$

$f(t) = f\left(d_{g1}/2\theta_{g1}(t) - d_{g2}/2\theta_{g2}(t) - e(t)\right)$ is the backlash function that simulates clearances; the actual transmission error is $x(t)-e(t)$; θ_{g1} and θ_{g2} are driver (pinion) and driven (gear) wheel positions; $T_{g1}(t)$ and $T_{g2}(t)$ are the driver and breaking torques; $T_{g2}(t) = T_{g1}d_{g2}/d_{g1}$; T_g is constant; d_{g1} and d_{g2} are the base gear diameters; I_{g1} and I_{g2} are rotary inertia; $e(t)$ represents the manufacturing error; when $e(t)$ is positive a lack of material is considered (see Fig. 2).

The gear mesh has a constant clearance equal to $2b$ along the line of action; the displacement function, that affects the restoring force, has the following expression:

$$f(x(t)-e(t)) = \begin{cases} x(t)-e(t)-b, & x(t)-e(t) \geqslant b, \\ 0, & |x(t)-e(t)| \leqslant b, \\ x(t)-e(t)+b, & x(t)-e(t) \leqslant -b. \end{cases} \tag{5}$$

Using Eq. (5) in Eq. (1), a second-order piecewise linear time varying differential equation is obtained.

Some authors (see e.g. Ref. [30]) suggested the use of smoothing techniques to apply standard numerical approaches in integrating equation (1). In the present work, the following smoothing function is considered:

$$\begin{aligned} f(t) \cong & \tfrac{1}{2}\{(x(t)-e(t)-b)[1+\tanh(\alpha(x(t)-e(t)-b))]\} \\ & + \tfrac{1}{2}\{(x(t)-e(t)+b)[1+\tanh(-\alpha(x(t)-e(t)+b))]\}, \end{aligned} \tag{6}$$

where $\alpha = 10^8$ is used for computations.

A 2D finite elements approach is applied to calculate the mesh stiffness; the software Calyx® is used to perform the analysis: such software uses a combined surface integral method and a finite element solution [31], which does not require mesh refinement close to the contact region.

If all teeth are perfect, the static transmission error, due to teeth flexibility, is periodic; its fundamental frequency is the mesh frequency. The stiffness $k(\theta)$ is obtained on static basis as follows:

$$k(\theta) = \frac{4T_{g1}}{d_{g1}^2 \delta(\theta)}, \tag{7}$$

where θ is the reference position of the pinion and $\delta(\theta)$ is the rigid body rotation of the pinion due to teeth flexibility.

The stiffness $k(\theta)$ is sampled within a mesh cycle; moreover, since the stiffness is periodic with the mesh frequency, its analytical formulation can be obtained by means of a Fourier expansion:

$$k(t) = k_0 + \sum_{i=1}^{N} k_i \cos(i\omega_m t - \varphi_i), \tag{8}$$

where $\omega_m = \omega_{g1} Z_1 = \omega_{g2} Z_2$ is the mesh angular frequency, Z_1 and Z_2 are pinion and gear number of teeth; ω_{g1} and ω_{g2} are the average rotational speeds of pinion and gear; amplitudes k_i and phases φ_i are obtained using the Discrete Fourier Transform (DFT) from a certain number n of stiffness samples within a mesh cycle.

In the following, the normalized amplitude $x/(2b)$ will be considered.

3. Composite profile errors

All processes used to manufacture gears suffer of a certain amount of deviation from the theoretical gear profile. In the present section, an iterative routine is described to create a random profile within the specified tolerance. Indeed, the actual profile error is generally measured using sophisticated and expensive experimental rigs; therefore, few data are available.

In simulating profile errors, it is important to define the profile tolerance (also referred to involute tolerance), which is the admissible amount of profile deviation from the theoretical profile. Since the profile geometry can be modified using tip or/and root relief, a particular chart, called K-chart is commonly used to specify the tolerance along the tooth profile, projected on the line of action. An example of K-chart, with both tip and root parabolic relief, is shown in Fig. 3. The chart provides the tolerance for each single profile segment vs. a coordinate (roll angle or diameter) along the tooth profile. Three segments are visible: the "tip relief segment" starting at the start-tip-roll-angle $\varphi_{t,s}$ with tolerance Δ_t, the "root relief segment" lying between the start-root-roll-angle $\varphi_{r,s}$ and the end-root-roll-angle $\varphi_{r,e}$ with tolerance Δ_r and the "involute segment" with tolerance Δ_i.

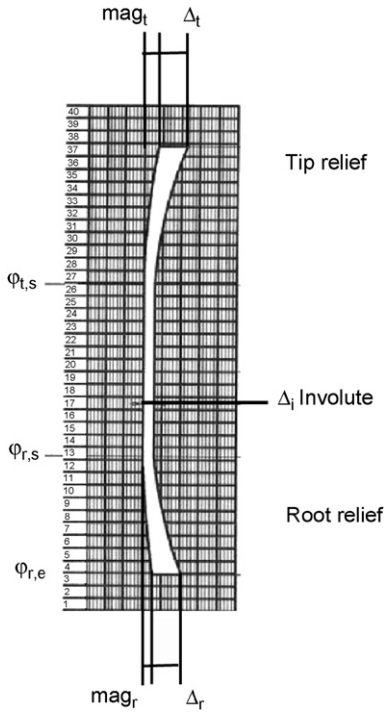

Fig. 3. Example of "K" chart.

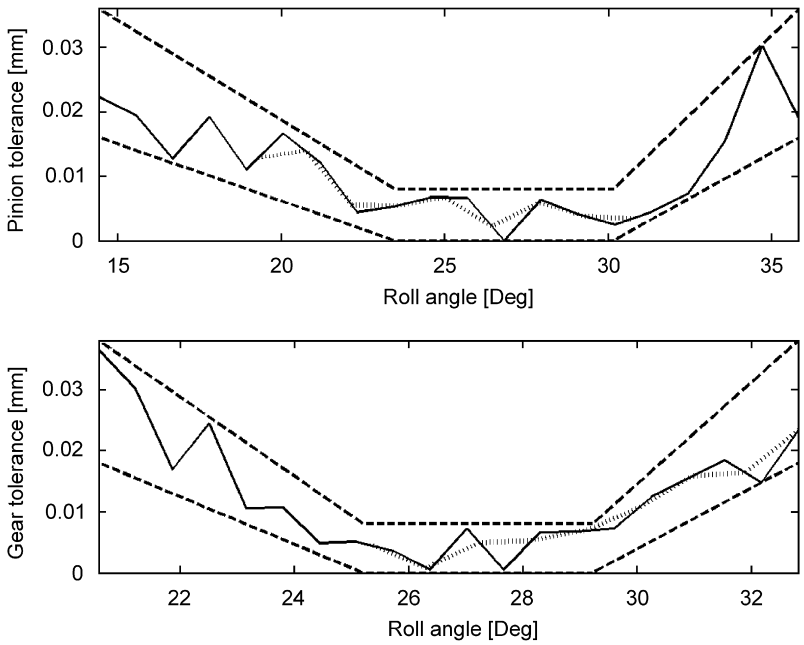

Fig. 4. Simulation of manufacturing errors according to "K" chart: (—) random data, (· · · ·) analytical expansion.

The quality inspection accepts a gear when the measured tooth profile lies between the lower and the upper allowance curves. Note that, at least one measured point must lie on the lower allowance curve to avoid the superposition of spacing errors.

The manufacturing quality can be simulated, according to the K-chart, in case of both linear or parabolic profile modification, by generating a random profile, which fits the K-chart. Fig. 4 shows an example of randomly generated profile, in the case of a linear tip and root relief. The present approach does not include further restriction on the profile curvature.

The deviation from the actual involute profile is provided with respect to the normalized roll angle $\varphi_n = 360(\varphi/\varphi_p)$, where ϕ is the actual roll angle and ϕ_p is the difference between the roll angle at the lowest and the highest points of contact along the tooth profile [32]. A positive value of deviation means lack of material.

The same approach is repeated to generate random profiles for all pinion and gear teeth. Once profile errors are randomly generated, an analytical formulation of the shape of each tooth profile error is expanded in Fourier series; it allows to evaluate the composite profile error, during a mesh cycle, as a sum of profile deviations of teeth in contact, according to the transmission ratio. This approach is repeated $Z_1 \times Z_2$ times in order to perform a complete fundamental rotation. The fundamental rotation allows two teeth in contact to return in the same relative position; this is the most general case, i.e. when Z_1 or Z_2 are prime numbers. During

Table 1
Complete geometrical data, profile modifications and tolerances (courtesy of CNH-Case New Holland)

Data	Pinion		Gear
Number of teeth	28		43
Module (mm)	3		3
Pressure angle (°)	20		20
Base radius (mm)	39.47		60.61
Theoretical pitch radius (mm)	42.00		64.50
Thickness on theoretical pitch circle (mm)	6.12		6.71
Addendum modification (mm)	1.93		2.75
Face width (mm)	20.00		20.00
Hob tip radius (mm)	0.90		0.90
Outer diameter (mm)	93.10		139.70
Root diameter (mm)	79.10		126.20
Inner diameter (mm)	40.00		40.00
Mass (kg)	0.72		1.98
Inertia ($kg\,m^2$)	0.0008		0.0048
Young's modulus (MPa)	206,000		206,000
Poisson's coefficient	0.3		0.3
Center distance (mm)		111.00	
Backlash (mm)		0.346	
Backlash ($2b$) on line of action (mm)		0.312	
Backside stiffness phase (rad)		1.5942	
Transmission ratio		0.65	
Contact ratio		1.29	
Involute tolerance (mm)	0.008		0.008
Tip relief			
Type of modification	Linear		Linear
Roll angle at start of relief (°)	30.157		29.213
Magnitude of relief (mm)	0.016		0.018
Tolerance (mm)	0.020		0.020
Root relief			
Type of modification	Linear		Linear
Roll angle at start of relief (°)	23.471		25.208
Roll angle at end of relief (°)	14.433		20.576
Magnitude of relief (mm)	0.016		0.018
Tolerance (mm)	0.020		0.020
Crowning			
Magnitude (mm)	None		None

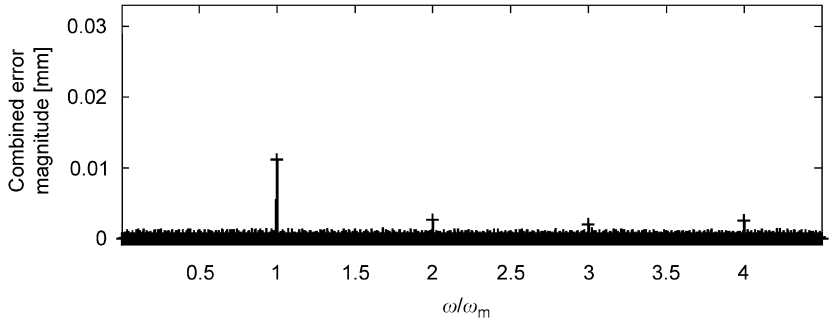

Fig. 5. Spectrum of the combined profile error.

such rotation, all possible relative teeth contact combinations take place, then the process is repeated periodically; therefore, the composite profile error is approximated again by means of a Fourier series:

$$e(t) = \sum_j E_j \cos(j\tilde{\omega}_m t - \gamma_j), \tag{9}$$

where: $\tilde{\omega}_m = \omega_m/(Z_1 Z_2)$ and E_j and γ_j are amplitudes and phases evaluated through the DFT.

The previous methodology is tested by means of the K-chart parameters described in Table 1; Fig. 4 shows a simulation of the manufacturing error for the first tooth of the pinion and the gear. Twenty measurements are simulated, the black line represents a possible machine measurement process. Using a Fourier expansion, ten points are used to calculate the combined profile deviation (dotted line in Fig. 4). Note that the extension of the dotted line, with respect to the roll angle, does not always coincide with the extension of the solid line; this is due to two reasons:

1. the start active profile radius can be different from the radius of the first contact point on the tooth profile;
2. the combined error for a single pair of teeth in contact is calculated in a mesh cycle; therefore, the last point considered is the highest one of single tooth contact.

Once the combined profile error is calculated for $Z_1 \times Z_2$ mesh cycles, the DFT algorithm provides the value of coefficients and phases for Eq. (9).

Fig. 5 shows an example of the composite profile error spectrum; all frequencies are normalized according to the mesh frequency ω_m. The effect of the profile error is an excitation having the most of energy localized at ω_m and its multiples; therefore, only such harmonics are considered. It is to note that the result of the generation process is a periodic function with pseudo-random amplitudes and phases.

It is worthwhile to stress that only manufacturing errors are included in $e(t)$; conversely, design (deterministic) profile modifications (root and tip relief) are modelled in the FEM analysis.

4. Validation

In this section, the procedure is validated by means of comparisons with the literature. Indeed, Eq. (1) has been deeply investigated and tested; however, it is well known that the evaluation of $k(t)$ is crucial and requires an accurate modelling of the wheel elasticity. The purpose of the present section is to show that the procedure followed to obtain Eq. (1) and its parameters is accurate.

Kahraman and Blankenship [6] presented several experiments on a gear pair with clearance, parametric and external forcing excitation. One of the tests were concerned with a spur gear set described in Table 2, with $\zeta = 0.01$ and $T_{g1} = 340\,\mathrm{N\,m}$.

Eq. (1) is numerically analysed using an adaptive step-size Gear integration algorithm that is suitable for stiff problems [33]. The present model gives: $\omega_n = 1.98 \times 10^4\,\mathrm{rad/s}$; using 15 positions in a mesh cycle, the peak to peak of the mesh stiffness is $6.24 \times 10^7\,\mathrm{N/m}$ and the peak to peak of the static transmission error is $5.35\,\mu\mathrm{m}$.

Table 2
Geometrical data of Ref. [6] spur gear set (courtesy of Prof. Kahraman)

	Pinion		Gear
Number of teeth	50		50
Module (mm)	3		3
Pressure angle (°)	20		20
Base diameter (mm)	140.95		140.95
Tooth thickness at pitch diameter (mm)	4.64		4.64
Outer diameter (mm)	156.00		156.00
Root diameter (mm)	140.68		140.68
Face width (mm)	20.00		20.00
Mass (kg)	2.52		2.52
Inertia (kg m^2)	0.0074		0.0074
Young's modulus (MPa)	206,000		206,000
Poisson's coefficient	0.3		0.3
Center distance (mm)		150.00	
Backlash (mm)		0.145	
Backlash ($2b$) on line of action (mm)		0.136	
Backside stiffness phase (rad)		1.5949	
Transmission ratio		1	
Contact ratio		1.7547	
Profile modifications		None	

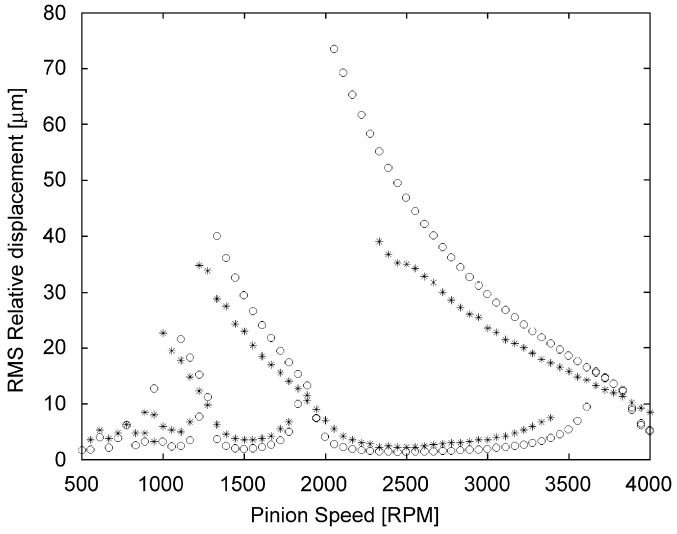

Fig. 6. Comparison between numerical simulation and experimental data: (○) Numerical simulation; (*) experimental data from Ref. [6].

The FEM simulation does not consider manufacturing errors $e(t) = 0$ and the stiffness function is approximated with 6 harmonics.

Fig. 6 shows the amplitude/frequency diagram for the present model and experimental results [6]: a good agreement is found.

5. Numerical results

In this section a case study is analysed in order to understand the effect of gear parameters on the dynamic behaviour.

Table 1 shows the geometrical and physical parameters of a spur gear pair; tip and root relief are given according to CNH s.p.a. standards. The nominal load of such gear pair is $T_{g1} = 470\,\mathrm{N\,m}$.

If tip and root relief are not considered (no profile modifications), the peak to peak of the mesh stiffness is 1.04×10^8 N/m, the peak to peak of the static transmission error is 11.65 μm and the natural frequency is $\omega_n = 3.16 \times 10^4$ rad/s. In presence of profile modifications, (Table 1), the peak to peak of the mesh stiffness is 3.12×10^7 N/m; the peak to peak of the static transmission error is 5.1 μm; the natural frequency is $\omega_n = 2.87 \times 10^4$ rad/s. Therefore, profile modifications reduce the peak to peak of both mesh stiffness and static transmission error (about 56%); moreover, the natural frequency of the system drops down (−9%). In this case, profile modifications do not change the main dynamic behaviour except for a general decrease of the vibration amplitude, because the setting of such profile modifications does not consider vibration aspects.

In the following, simulations are carried with $\zeta = 0.01$.

5.1. Effect of manufacturing errors

In the gear pair described in Table 1, manufacturing errors can be modelled using the procedure outlined in Section 3 and tolerance data of Table 1, see also Fig. 4. The *DFT* of the combined profile error is expanded using four harmonics (see Fig. 5 and Table 3).

Fig. 7 shows that manufacturing errors do not change the qualitative dynamic behaviour, but induce a considerable vibration amplitude increase at all frequencies. This behaviour is more evident at low speeds, where contact loss can also occur. In Fig. 7 the thick line represents the dynamics of the gear pair with tip and root relief, without manufacturing errors; the thin line represents the same case with manufacturing errors obtained from the stochastic approach outlined in Section 3 (Table 1).

Table 3
Components of the stochastically simulated manufacturing profile error; gear data in Table 1

ω_m/ω_n	Normalized manufacturing error components		Phase (rad)	
1	$\overline{E_1}$	6.88×10^{-2}	γ_1	9.35×10^{-1}
2	$\overline{E_2}$	1.87×10^{-2}	γ_2	1.99
3	$\overline{E_3}$	1.75×10^{-2}	γ_3	2.52
4	$\overline{E_4}$	1.60×10^{-2}	γ_4	2.88

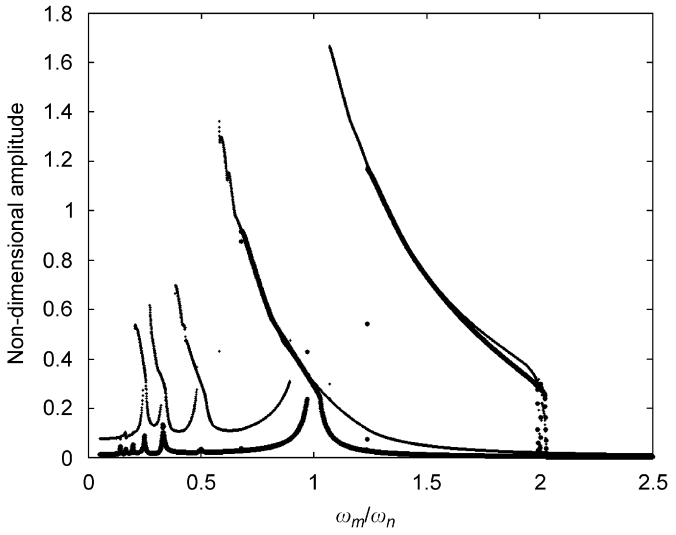

Fig. 7. Comparison of amplitude–frequency diagrams: no manufacturing errors (thick line); with manufacturing errors (thin line); gear data in Table 1.

Table 4
Components of the stochastically simulated manufacturing profile error; gear data in Table 1

ω_m/ω_n	Normalized manufacturing error components		Phase (rad)	
1	$\overline{E_1}$	6.73×10^{-2}	γ_1	9.60×10^{-1}
2	$\overline{E_2}$	1.68×10^{-2}	γ_2	2.01
3	$\overline{E_3}$	1.68×10^{-2}	γ_3	2.01
4	$\overline{E_4}$	1.38×10^{-2}	γ_4	2.97

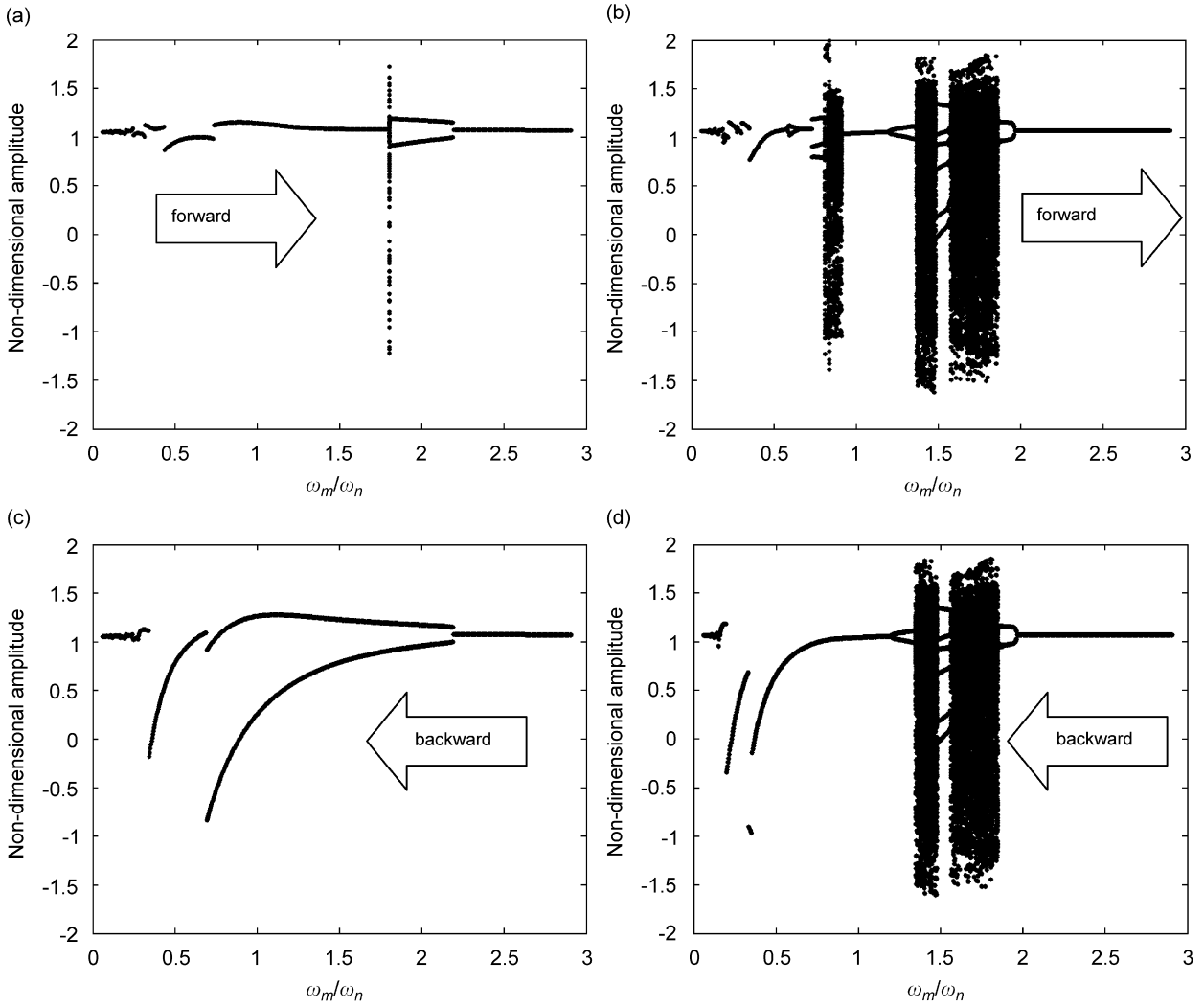

Fig. 8. Comparison of bifurcation diagrams: (a) forward with no manufacturing errors; (b) forward with manufacturing errors; (c) backward with no manufacturing errors; and (d) backward with manufacturing errors; gear data in Tables 1 and 3.

A further analysis has been carried out considering several set of simulated manufacturing errors with the same tolerance class (Table 1); indeed, the stochastic process does not lead to a unique set of profile errors. Ten simulations are performed, the average of the composite profile error rms is 0.018 mm with a variance equal to 1.44×10^{-8} mm. Dynamic analyses, carried out on such cases, have been post-processed considering

the dynamic scenario, see e.g. Fig. 7; the maximum amplitude of oscillation, over the entire excitation spectrum, has been considered; the average of maxima is $1.45 \times 2b$ and the maximum of maxima is $1.71 \times 2b$. This shows the importance of a statistical approach; indeed, even though the variance of profile errors is small, the effect on the dynamics is not negligible; therefore, a single analysis could underestimate the effect of manufacturing errors.

5.2. Chaotic behaviour

Simulations are now performed at very low torque, $T_{g1} = 100$ N m, the natural frequency is $\omega_n = 2.52 \times 10^4$ rad/s, the peak to peak of the mesh stiffness and the static transmission error are

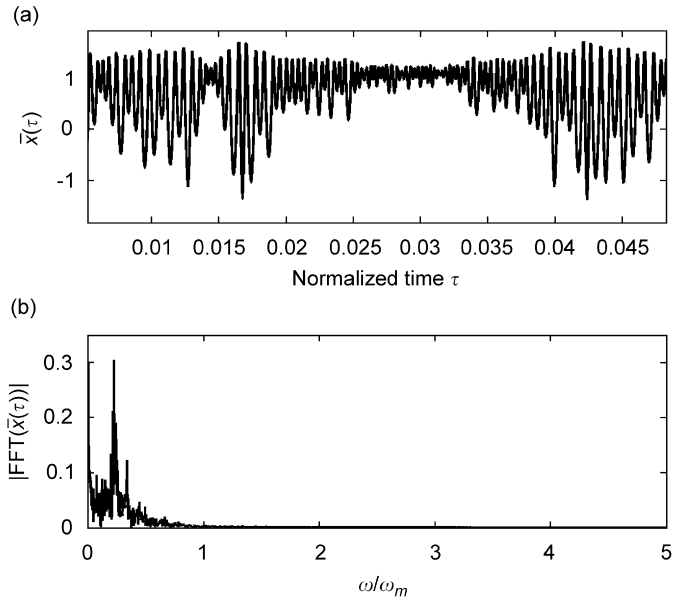

Fig. 9. Time history and relative spectrum at $\omega_m/\omega_n = 1.70$; gear data in Tables 1 and 4.

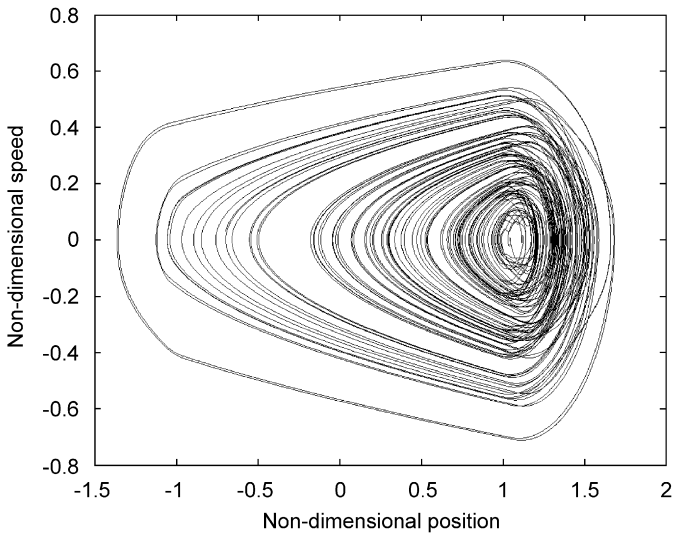

Fig. 10. Phase plane plot at $\omega_m/\omega_n = 1.70$; gear data in Tables 1 and 4.

1.59×10^8 N/m and 13.54 μm, respectively. Two analyses are carried out with and without manufacturing errors (Table 4).

Fig. 8 shows that a chaotic vibration appears only when manufacturing errors are included in the model; there is only an extremely narrow region of chaos in absence of manufacturing errors; conversely, wide chaotic regions are found in presence of manufacturing errors; this is in agreement with experiments of Ref. [6]. Chaotic regions are alternated with 2 and 6 T regions and the route to the chaos is a "blue sky catastrophe" type. A time history is computed for $\omega_m/\omega_n = 1.7021$. The response, its spectrum (Fig. 9) and the phase plane plot (Fig. 10) confirm the chaotic behaviour of the system: intermittency is evidenced, as well as a narrow band continuous spectrum (which indicates low-dimensional chaos); the phase-space representation shows that a region is completely filled by the phase trajectory.

6. Conclusions

The nonlinear dynamics of spur gears with manufacturing errors is analysed by means of a one-degree-of-freedom system that includes time varying stiffness, backlash and profile errors. The stiffness has been obtained on static basis by means of a finite element analysis, which takes into account the nonlinearity due to the contact and profile modification such as tip and root relief. A stochastic approach is developed to simulate manufacturing errors, when only the profile tolerance (K-chart) is known. This technique allows performing dynamics simulation once design and manufacturing parameters are provided.

The presence of manufacturing errors magnifies the amplitude of vibration and leads to chaotic vibrations in a wide range of rotation speed when the external torque is small. Chaos is associated to high amplitude of oscillation and a wide band spectrum response.

The stochastic approach shows that slightly different profile errors, within the same tolerance class, can lead to differences in terms of amplitude of oscillation that are not negligible. This justifies the use of the stochastic approach and suggests to carry out several simulations to determine the statistical dynamic behaviour.

The use of measured errors gives more realistic information; however, a large set of gear pairs have to be measured in order to obtain a full statistical error distribution. Indeed, in the present work it is proved that using only a single measured set could lead to unreliable prediction of the dynamic behaviour, due to the high sensitivity of the gear response on profile error variations.

Acknowledgements

The authors thank: Case New Holland (Italy) and SIMECH Lab. for supporting the present research; Advanced Numerical Solutions (USA) for providing the software CALYX®; Professor Kahraman for supplying experimental data.

References

[1] S.L. Harris, Dynamic loads on the teeth of spur gears, *Proceedings of the Institution of Mechanical Engineers* 172 (2) (1958) 87–100.
[2] R.W. Gregory, S.L. Harris, R.G. Munro, Dynamic behavior of spur gears, *Proceedings of the Institution of Mechanical Engineers* 178 (1963–1964) 207–218.
[3] H. Walker, Gear tooth deflection and profile modification, *The Engineer* 14 (1938) 409–412.
[4] W.D. Mark, Analysis of the vibratory excitation of gear systems: basic theory, *Journal of Acoustical Society of America* 63 (5) (1978) 1409–1430.
[5] C.H. Chung, G. Steyer, T. Abe, M. Clapper, C. Shah, Gear noise reduction through transmission error control and gear blank dynamic tuning, *Proceedings of the 1999 Noise and Vibration Conference*, SAE Technical Paper 1999-01-1766, 1999.
[6] A. Kahraman, G.W. Blankenship, Experiments on nonlinear dynamic behavior of an oscillator with clearance and periodically time-varying parameters, *Journal of Applied Mechanics* 64 (1997) 217–226.
[7] H.N. Ozguven, D.R. Houser, Mathematical models used in gear dynamics—a review, *Journal of Sound and Vibration* 121 (3) (1988) 383–411.
[8] C.S. Hsu, W.-H. Cheng, Steady-state response of a dynamical system under combined parametric and forcing excitations, *Journal of Applied Mechanics* (1974) 371–378.
[9] M. Benton, A. Seireg, Simulation of resonances and instability conditions in pinion-gear systems, *Journal of Mechanical Design* 100 (1978) 26–32.

[10] C.C. Wang, Rotational vibration with backlash: part 1, *Journal of Mechanical Design* 100 (1978) 363–373.
[11] C.C. Wang, Rotational vibration with backlash: part 2, *Journal of Mechanical Design* 103 (1981) 387–409.
[12] Y. Cai, Simulation on the rotational vibration of helical gears in consideration of the tooth separation phenomenon (a new stiffness function of helical involute tooth pair), *Journal of Mechanical Design* 117 (1995) 460–469.
[13] A. Kahraman, R. Singh, Non-linear dynamics of a spur gear pair, *Journal of Sound and Vibration* 142 (1) (1990) 49–75.
[14] M. Amabili, A. Rivola, Dynamic analysis of spur gear pairs: steady-state response and stability of sdof model with time-varying meshing damping, *Mechanical Systems and Signal Processing* 11 (3) (1997) 375–390.
[15] A. Kahraman, R. Singh, Dynamics of an oscillator with both clearance and continuous non-linearities, *Journal of Sound and Vibration* 151 (3) (1992) 180–185.
[16] G.W. Blankenship, A. Kahraman, Steady state forced response of a mechanical oscillator with combined parametric excitation and clearance type non-linearity, *Journal of Sound and Vibration* 185 (5) (1995) 743–765.
[17] A. Kahraman, G.W. Blankenship, Interactions between commensurate parametric and forcing excitations in a system with clearance, *Journal of Sound and Vibration* 194 (3) (1996) 317–336.
[18] S. Natsiavas, Periodic response and stability of oscillators with symmetric trilinear restoring force, *Journal of Sound and Vibration* 134 (2) (1989) 315–331.
[19] G.R. Tomlinson, J. Lam, Frequency response characteristics of structures with single and multiple clearance-type non-linearity, *Journal of Sound and Vibration* 96 (1) (1984) 111–125.
[20] S. Theodossiades, S. Natsiavas, Non-linear dynamics of gear-pair systems with periodic stiffness and backlash, *Journal of Sound and Vibration* 229 (2) (2000) 287–310.
[21] H.N. Ozguven, A non-linear mathematical model for dynamic analysis of spur gears including shaft and bearing dynamics, *Journal of Sound and Vibration* 145 (2) (1991) 239–259.
[22] R.G. Munro, Effect of geometrical errors on the transmission of motion between gears, *Proceedings of the Institution of Mechanical Engineers* 184 (30) (1969–1970) 79–84.
[23] K. Umezawa, Y. Sato, K. Kohno, Influence of gear errors on rotational vibration of power transmission spur gear (1st report pressure angle and normal pitch error), *Bulletin of Japanese Society of Mechanical Engineering* 27 (225) (1984) 569–575.
[24] K. Umezawa, Y. Sato, Influence of gear errors on rotational vibration of power transmission spur gear (2nd report waved form error), *Bulletin of Japanese Society of Mechanical Engineering* 28 (243) (1985) 2143–2148.
[25] P. Velex, M. Maatar, A mathematical model for analyzing the influence of shape deviations and mounting errors on gear dynamic behaviour, *Journal of Sound and Vibration* 191 (5) (1996) 629–660.
[26] W.D. Mark, Analysis of the vibratory excitation of gear systems. II: Tooth error representation, approximations, and application, *Journal of Acoustical Society of America* 66 (6) (1979) 1758–1787.
[27] M. Ognjanovic, A. Subic, Gear quality prediction using vibration analysis, *Machine Vibration* 2 (1993) 92–100.
[28] Y. Cai, T. Hayashi, The linear approximated equation of vibration of a pair of spur gears (theory and experiment), *Journal of Mechanical Design* 116 (1994) 558–564.
[29] T. Hayashi, I. Hayashi, The rotational vibration of a spur gear with tooth profile error, *Bulletin of Research Laboratory of Precision Machinery and Electronics, Tokyo Institute of Technology* 38 (1976) 35–42.
[30] T.C. Kim, T.E. Rook, R. Singh, Effect of smoothening functions on the frequency response of an oscillator with clearance non-linearity—Letter to the Editor, *Journal of Sound and Vibration* 263 (3) (2003) 665–678.
[31] S.M. Vijayakar, A combined surface integral and finite element solution for a three-dimensional contact problem, *International Journal for Numerical Methods in Engineering* 31 (1991) 525–545.
[32] D.W. Dudley, D.P. Townsend, *Dudley's Gear Handbook*, McGraw-Hill, Inc., New York, USA, 1992.
[33] IMSL®, *IMSL Fortran Library User's Guide, MATH/LIBRARY*, Vols. 1 and 2, Visual Numerics Inc., USA, 2003.